Sensor and Simulation Notes
Note 360
July 22, 1993

A Uniform Dielectric Lens for Launching a Spherical Wave into a Paraboloidal Reflector

Carl E. Baum

and

Joseph J. Sadler

Phillips Laboratory

and

Alexander P. Stone

Phillips Laboratory and

University of New Mexico

Abstract

In this paper we consider dielectric-lens designs for the specific case of launching an approximate spherical TEM wave onto an impulse radiating antenna (IRA). Restrictions on launch angles are derived yielding a range of acceptable lens parameters. An equal transit-time condition on ray paths is imposed to ensure the correct spherical wavefront. Some reflections, ideally small, at the lens boundary are allowed. Illustrations and numerical tables are presented from which examples of these lenses may be constructed.

CLEARED
FOR PUBLIC RELEASE
PL/PA
8-6-93

PL93-0539

1 Introduction

Consider an impulse radiating antenna (IRA) in the form of a paraboloidal reflector fed by a conical transmission line suitable for guiding a spherical TEM wave [1] as indicated in Fig. 1.1. The paraboloidal reflector is assumed to have a circular edge of radius a with

$$D = 2a \equiv \text{ diameter} \tag{1.1}$$

The apex of the conical feed is located a distance

$$F \equiv \text{ focal distance} \tag{1.2}$$

from the center of the reflector. As discussed in [2] the angle from the apex of the conical transmission line (focal point) to the edge of the reflector is

$$\begin{aligned} \theta_{2_{\max}} &= \operatorname{arccot}\left(\frac{2F}{D} - \frac{D}{8F}\right) = 2\arctan\left(\frac{D}{4F}\right) \\ &= 2\arctan\left(\frac{a}{2F}\right) \end{aligned} \tag{1.3}$$

If, as an example of commonly used reflector parameters $F/D = 0.4$, then we have $\theta_{2_{\max}} \simeq 64.01°$. Centering our coordinate system on the conical apex, then $0 \leq \theta_2 \leq \theta_{2_{\max}}$ represents the range of interest of angles for launching an electromagnetic wave toward the reflector, the axis of rotation symmetry of this reflector being taken as the z axis in the usual spherical coordinates.

As discussed in [2], as one extrapolates the desired wave on the TEM launch back toward the apex the electric field is larger and larger, until at some position before reaching the apex electrical breakdown conditions are exceeded. This is especially important in transmission where high voltages (and corresponding high powers) are desired. If the required spacing of the conical conductors at this cross section is larger than radian wavelengths at the highest frequencies of interest, or larger than some small rise time (times the speed of light) of interest, then particular care needs to be taken in synthesizing the fields at this cross section

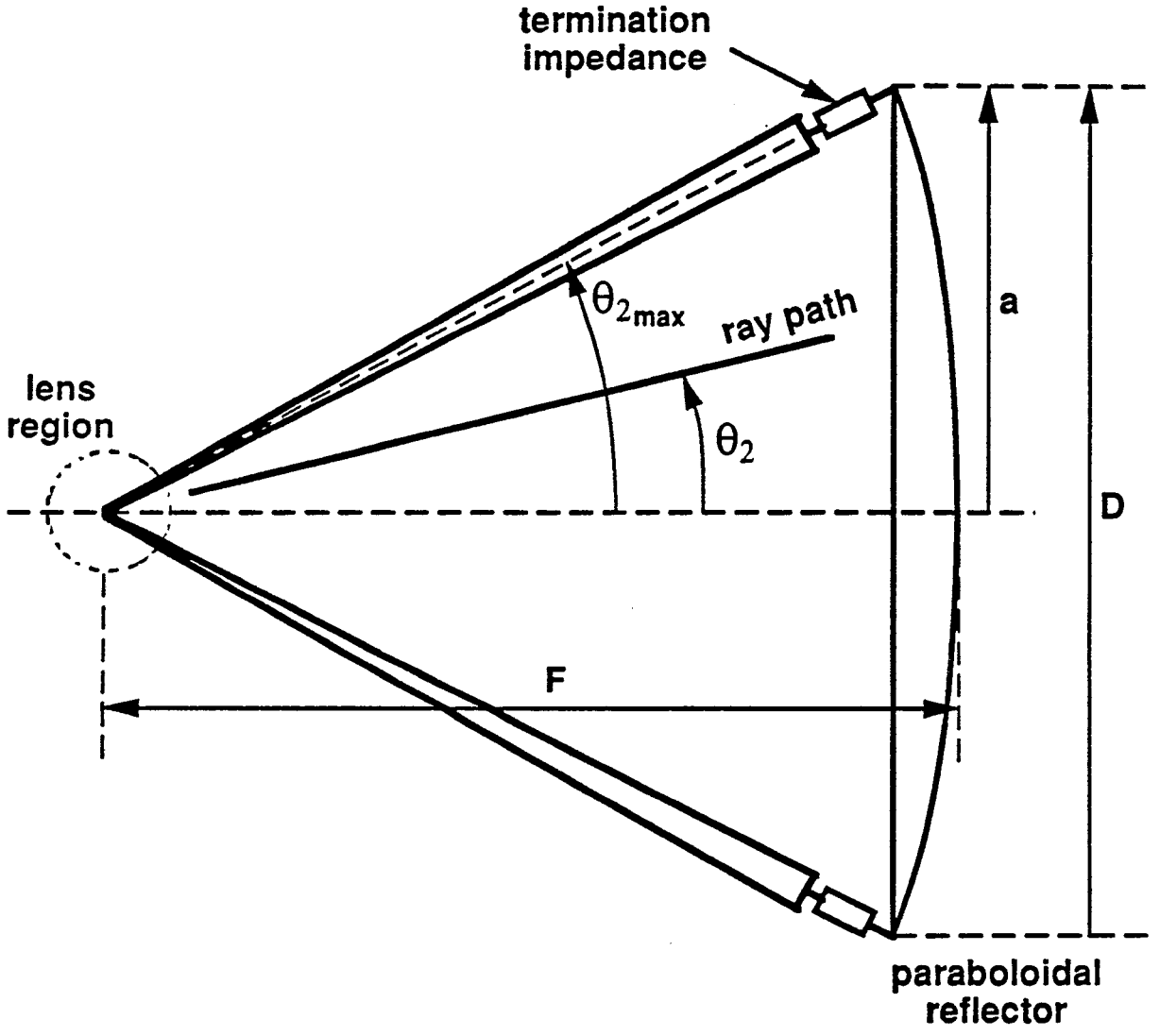

Fig. 1.1: Reflector IRA

(on some aperture spherical surface). One way to achieve the increased dielectric strength, allowing one to extrapolate the desired wave back to smaller cross sections, where a switch or some other appropriate electrical source is located, is by the use of a dielectric lens. Various kinds of lenses can be considered, including those which in an ideal sense can launch the exact form of spherical TEM wave desired [7]. Here we consider a simple uniform dielectric lens which meets the equal-time requirement for the desired spherical wave, but has some (preferably small) reflections at the lens boundary which distort somewhat the desired spatial distribution (TEM) of the fields on the aperture sphere.

The lens region in Fig. 1.1 is shown on an expanded scale in Fig. 1.2. In the notation of [5] the apex, or focal point for the spherical wave (outside the lens) launched toward the reflector, is the origin ($\vec{r}_2 = \vec{0}$) of the $\vec{r}_2$ coordinate system. Here we illustrate some cut at a constant ϕ, the lens being a body of revolution. Defining

$$\epsilon_r \equiv \frac{\epsilon_1}{\epsilon_2} \equiv \text{ relative permeability of lens} \tag{1.4}$$

we let the permeability both inside and outside the lens be μ_0. The outer permittivity ϵ_2 will often be taken as ϵ_0 in practical cases, and the lens permittivity ϵ_1 will be taken as that for dielectrics of interest such as for polyethylene or transformer oil (i.e. 2.26).

The $\theta_{2_{max}}$ previously introduced is now the maximum of θ_2, describing the rays leaving the lens toward the reflector. Inside the lens there are rays emanating from $(x, y, z) = (0, 0, \ell_2 - \ell_1)$ with the angle θ_1 with respect to the z axis. With the inside and outside rays meeting at the lens boundary the various angles are related. Corresponding to $\theta_{2_{max}}$ there is also a $\theta_{1_{max}}$ with $0 \leq \theta_1 \leq \theta_{1_{max}}$. For normalization purposes the position on the lens boundary for this outermost ray of interest is defined as having a cylindrical radius h. For later use this position will remain fixed for a given $\theta_{2_{max}}$ for various shapes of the lens boundary given by varying $\theta_{1_{max}}$. Note that the scaling lengths in [5] are related by the focal-length formula

$$\ell_0^{-1} = \ell_1^{-1} + \ell_2^{-1} \tag{1.5}$$

So given ℓ_1 and ℓ_2 one finds ℓ_0 for use in the formulas of [5], and ℓ_0 is scaled in units of h.

$\theta_{1_{max}} = 70°$ $\qquad \frac{\ell_2 - \ell_1}{h} = 0.12$

$\theta_{2_{max}} = 64.0°$

$\varepsilon_r = 2.26$ $\qquad \frac{\ell_2}{h} = 1.35$

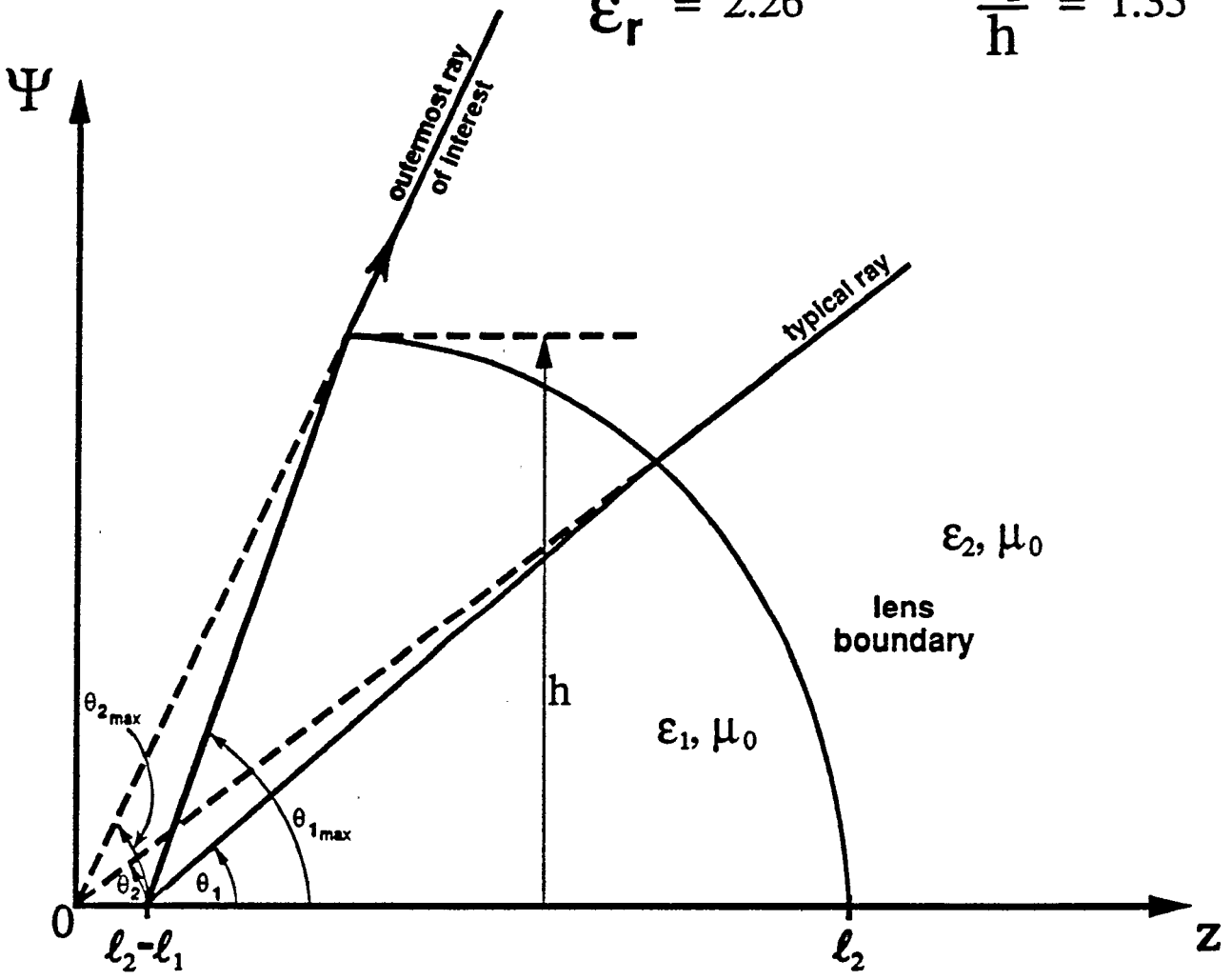

Fig. 1.2: Lens For Launching Spherical Wave

2 Restrictions on Launch Angles

As indicated in Fig. 2.1 there is a potential problem with the lens concerning the fatness (extent of cylindrical radius Ψ) and the maximum angle $\theta_{2_{max}}$ for launching the spherical wave outside the lens. In particular as θ_2 approaches $\theta_{2_{max}}$ from below, the lens boundary should not cross over the outermost ray of interest defined by $\theta_2 = \theta_{2_{max}}$. Referring to Fig. 2.1 then we require that the slope of the lens boundary, where the boundary meets this ray, should satisfy

$$\theta_{\ell_{max}} \leq \theta_{2_{max}} \tag{2.1}$$

Note that the radius of the lens boundary Ψ_b can be allowed to exceed h, still meeting the restriction of (2.1).

Take the limit of equality in (2.1) to define critical angles (subscript "c").. This case is illustrated in Fig. 2.2, where the region where the critical ray meets the boundary is expanded. Appealing to Snell's law in which the phase velocities of the waves in the two media are matched along the boundary gives

$$\sqrt{\epsilon_1}\sin(\psi_i) = \sqrt{\epsilon_2}\sin(\psi_t) \tag{2.2}$$

Setting

$$\theta_{\ell_c} = \theta_{2_c} \tag{2.3}$$

then we have

$$\psi_t = \frac{\pi}{2} \tag{2.4}$$

i.e., the wave in medium 2 is propagating parallel to the lens boundary. By geometric construction we have

$$\psi_i = \frac{\pi}{2} + \theta_{2_c} - \theta_{1_c} \tag{2.5}$$

which gives

$\theta_{1_{max}} = 80°$ $\quad \frac{\ell_2 - \ell_1}{h} = 0.3$

$\theta_{2_{max}} = 64.0°$

$\varepsilon_r = 2.26$ $\quad \frac{\ell_2}{h} = 1.75$

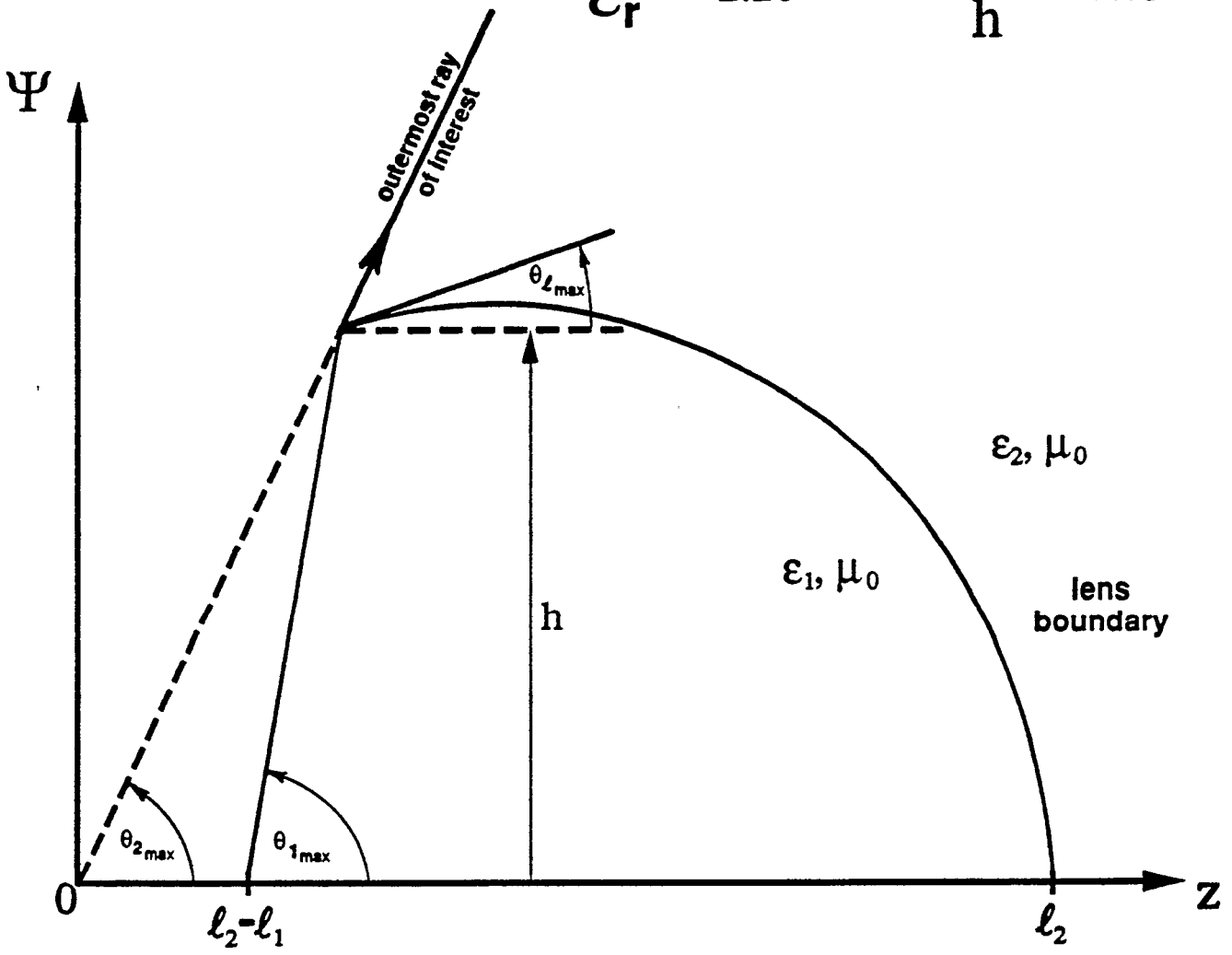

Fig. 2.1: Restriction of Lens Boundary to Inside Outermost Ray of Interest

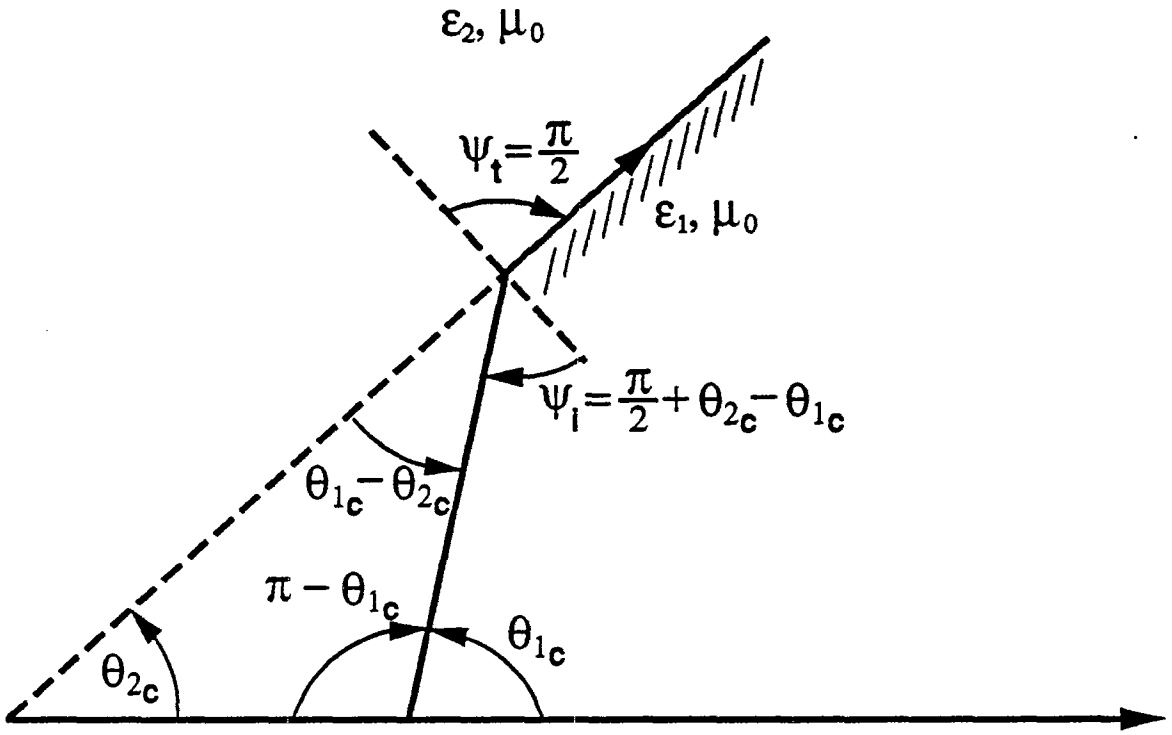

Fig. 2.2: Critical Angle of Lens Boundary

$$\begin{aligned}\sin\left(\frac{\pi}{2}+\theta_{2_c}-\theta_{1_c}\right) &= \cos(\theta_{2_c}-\theta_{1_c}) = \cos(\theta_{1_c}-\theta_{2_c}) \\ &= \epsilon_r^{-\frac{1}{2}} \\ \theta_{1_c} &= \theta_{2_c} + \arccos(\epsilon_r^{-\frac{1}{2}})\end{aligned} \tag{2.6}$$

where one needs the principle value for the arccos noting that $\theta_{1_c} > \theta_{2_c}$ in the construction of Fig. 2.2.

Noting in (2.2) that a transmission angle $\psi_t \leq \pi/2$ gives $\theta_{\ell_{\max}} \leq \theta_{2_{\max}}$ as an acceptable lens boundary in Fig. 2.1, then we have

$$\begin{aligned}\sin(\psi_i) = \sin\left(\frac{\pi}{2}+\theta_{2_{\max}}-\theta_{1_{\max}}\right) &= \cos(\theta_{1_{\max}}-\theta_{2_{\max}}) \\ \geq \epsilon_r^{-\frac{1}{2}} & \\ \theta_{1_{\max}} - \theta_{2_{\max}} &\leq \arccos(\epsilon_r^{-\frac{1}{2}}) \\ \theta_{1_{\max}} &\leq \theta_{2_{\max}} + \arccos(\epsilon_r^{-\frac{1}{2}})\end{aligned} \tag{2.7}$$

Now we can also allow $\theta_{1_{\max}} < \theta_{2_{\max}}$, but then the geometrical construction in Figs. 2.1 and 2.2 do not apply and the lens boundary becomes concave to the right [5]. For present considerations, since $\theta_{1_{\max}}$ describes the path of the conical-transmission-line conductors in the lens region, a region which lowers the characteristic impedance from that of the conical transmission line outside the lens, our interest centers on $\theta_{1_{\max}}$ near $\pi/2$ which maximizes the transmission -line characteristic impedance in the lens. There are other considerations as well, such as high voltages (breakdown) in the lens near the conical apex at $(x, y, z) = (0, 0, \ell_2 - \ell_1)$, which push in the same direction. So for this paper our attention concerning $\theta_{1_{\max}}$ is limited to

$$\theta_{2_{\max}} \leq \theta_{1_{\max}} \leq \min\left[\frac{\pi}{2}, \theta_{2_{\max}} + \arccos(\epsilon_r^{-\frac{1}{2}})\right] \tag{2.8}$$

For our example cases

$$\begin{aligned}\epsilon_r &= 2.26 \\ \arccos\ (\epsilon_r^{-\frac{1}{2}}) &\simeq 48.3^\circ\end{aligned} \tag{2.9}$$

Note that for large ϵ_r the allowable range of $\theta_{1_{\max}}$ is constrained close to $\theta_{2_{\max}}$.

3 Special Case of $\theta_1 = \theta_2$: Spherical Lens

A very simple lens is that of a sphere of radius b centered on the origin with

$$\begin{aligned} \ell_2 &= \ell_1 = 2\ell_0 = b \\ \theta_2 &= \theta_1,\ \theta_{2_{\max}} = \theta_{1_{\max}} \end{aligned} \tag{3.1}$$

In this case, if the conical transmission line in medium 2 has a characteristic impedance Z_{c_2}, then continuing the conical conductors back into the lens gives a characteristic impedance there of

$$Z_{c_1} = \epsilon_r^{-\frac{1}{2}} Z_{c_2} \tag{3.2}$$

While the TEM modal distribution is the same on both sides of the lens boundary there is a reflection at the boundary with reflection coefficient

$$R = \frac{Z_{c_2} - Z_{c_1}}{Z_{c_2} + Z_{c_1}} = \frac{\epsilon_r^{\frac{1}{2}} - 1}{\epsilon_r^{\frac{1}{2}} + 1} \tag{3.3}$$

and transmission coefficient

$$T = 1 + R = \frac{2\epsilon_r^{\frac{1}{2}}}{\epsilon_r^{\frac{1}{2}} + 1} \tag{3.4}$$

For our example case we have

$$\begin{aligned} \epsilon_r &= 2.26 \\ R &\simeq 0.20, \quad T \simeq 1.20 \end{aligned} \tag{3.5}$$

The reflected wave in turn reflects off the source point (apex) with an amplitude dependent on the source impedance, say -1 reflection for a short circuit. This reflection in turn passes through the lens boundary as another spherical TEM wave.

Note that in principle the lens should be a complete sphere (4π steradians, volume $4\pi b^3/3$) for the above analysis to exactly apply. Otherwise the missing portions of the lens can introduce other modes which affect the fields at the observer with $\theta \leq \theta_2 \leq \theta_{2_{\max}}$, complicating the waveform during the times of significance for the reflections.

This points to a possible disadvantage for this kind of spherical lens. Other lens shapes, while meeting the equal-time requirement for the first wave through the lens going into a spherical wave outside the lens, can break up the wavefront for successive waves by sending non-spherical waves back from the lens boundary which need not (in large part) converge on the source point.

4 Brewster-Angle Considerations

One can reduce reflections at the lens boundary by changing the direction of incidence for appropriate polarization (E wave) by use of Brewster angle considerations [3, 4, 6]. Referring to Fig. 4.1, and using a subscript "B" for this case we have

$$\begin{aligned}
\cos(\psi_{iB}) &= \left[\frac{\epsilon_r}{\epsilon_r + 1}\right]^{\frac{1}{2}} = \sin(\psi_{tB}) \\
\sin(\psi_{iB}) &= [\epsilon_r + 1]^{-\frac{1}{2}} = \cos(\psi_{tB}) \\
\cot(\psi_{iB}) &= \epsilon_r^{\frac{1}{2}} = \tan(\psi_{tB}) \\
\psi_{iB} + \psi_{tB} &= \frac{\pi}{2} = 90^\circ
\end{aligned} \tag{4.1}$$

For our example case we have

$$\begin{aligned}
\epsilon_r &= 2.26 \\
\psi_{iB} &\simeq 33.6^\circ \\
\psi_{tB} &\simeq 56.4^\circ
\end{aligned}$$

Noting that the angle ψ_{tB} of the transmitted ray is greater than 0° (transmission of normally incident wave) but less than 90° (corresponding to transmission parallel to the lens boundary as in Fig. 2.2), then for $\theta_{1_{max}}$ chosen near the critical case there are $\theta_1 < \theta_{1\,max}$ and $\theta_2 < \theta_{2_{max}}$ which satisfy this Brewster-angle condition. So increasing $\theta_{1_{max}}$ above $\theta_{2_{max}}$ as in (2.8) can make some of the rays have a better transmission through the lens boundary.

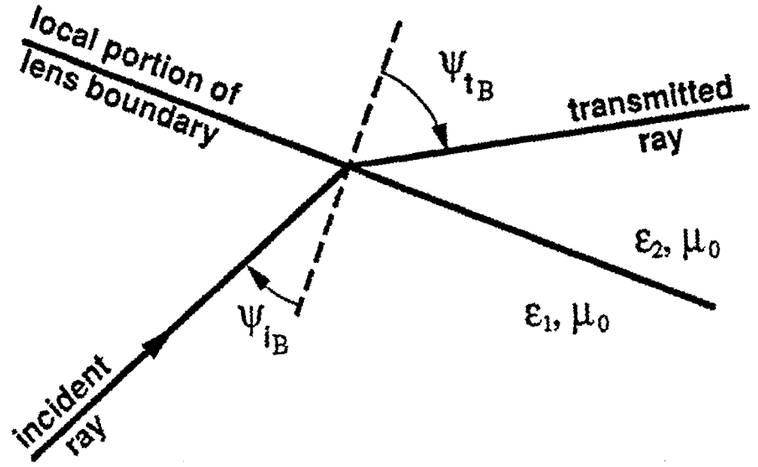

Fig. 4.1: Total Transmission of E Wave at Brewster Angle

5 Lens Shapes

The equal-time condition for a diverging spherical wave in a medium with permittivity ϵ_1 going into another diverging spherical wave in a second medium with permittivity ϵ_2 is given by the equation

$$\sqrt{\epsilon_1}\Big\{\big[[z_b-\ell_2+\ell_1]^2+\Psi_b^2\big]^{\frac{1}{2}}-\ell_1\Big\}=\sqrt{\epsilon_2}\Big\{\big[z_b^2+\Psi_b^2\big]^{\frac{1}{2}}-\ell_2\Big\} \tag{5.1}$$

where ℓ_1, ℓ_2, z_b and Ψ_b are as in Fig. 1.2. This expression is derived in [5] where it appears as (4.9). If we use the coordinate relations on the lens boundary, given by

$$z_b-\ell_2=\Psi_b\cot(\theta_{1_b})-\ell_1=\Psi_b\cot(\theta_{2_b})-\ell_2 \tag{5.2}$$

the equal-time condition can then be re-expressed in the form

$$\Big(\frac{\ell_2}{\ell_1}-\epsilon_r^{\frac{1}{2}}\Big)\Big[\sin(\theta_{1_b})\cos(\theta_{2_b})-\cos(\theta_{1_b})\sin(\theta_{2_b})\Big]=\Big(\frac{\ell_2}{\ell_1}-1\Big)\Big[\sin(\theta_{1_b})-\epsilon_r^{\frac{1}{2}}\sin(\theta_{2_b})\Big] \tag{5.3}$$

where $\epsilon_r=\epsilon_1/\epsilon_2$. There are also constraints on θ_1 and θ_2, derived in the earlier sections of this paper, and these are

$$\begin{aligned}\theta_{1_{\max}} &\le \theta_{2_{\max}}+\arccos(\epsilon_r^{-\frac{1}{2}})\\ \theta_{2_{\max}} &\le \theta_{1_{\max}} \le \min\Big[\frac{\pi}{2},\theta_{2_{\max}}+\arccos(\epsilon_r^{-\frac{1}{2}})\Big]\end{aligned} \tag{5.4}$$

Since $\theta_{2_{\max}}=2\arctan(\frac{D}{4F})$ from (1.3), we may choose various F/D ratios to determine lens shapes. Thus, for a given F/D value, $\theta_{2_{\max}}$ is determined. If we then choose h (Fig. 1.2) and ϵ_r and $\theta_{1_{\max}}$ consistent with our constraints, we obtain the lens parameters ℓ_1/h and ℓ_2/h. Since θ_2 is a function of θ_1 (or vice versa) a lens boundary curve is generated for given $\epsilon_r, \ell_1/h$, and ℓ_2/h with $\theta \le \theta_1 \le \theta_{1_{\max}}$, $0 \le \theta_2 \le \theta_{2_{\max}}$. If we now select a new $\theta_{1_{\max}}$, another lens can be specified for our choice of F/D. Thus by varying F/D a large collection of lens designs are obtainable.

The process described above will now be analyzed in detail. Let us fix $\theta_{2_{\max}}$ (via choice of F/D), choose h and select $\theta_{1_{\max}}$ in accordance with the constraints (5.4). The parameters

ℓ_1/h and ℓ_2/h are determined by the transit-time relation and we find that

$$\frac{\ell_2}{\ell_1} = \frac{\epsilon_r^{\frac{1}{2}}\left[\sin\left(\theta_{1_{\max}} - \theta_{2_{\max}}\right) + \sin\left(\theta_{2_{\max}}\right)\right] - \sin\left(\theta_{1_{\max}}\right)}{\sin\left(\theta_{1_{\max}} - \theta_{2_{\max}}\right) + \epsilon_r^{\frac{1}{2}}\sin\left(\theta_{2_{\max}}\right) - \sin\left(\theta_{1_{\max}}\right)} \tag{5.5}$$

Since the geometry indicated in Fig. 1.2 gives the relation

$$\frac{\ell_2 - \ell_1}{h} = \cot(\theta_{2_{\max}}) - \cot(\theta_{1_{\max}}) \tag{5.6}$$

we can find explicit formulas for ℓ_1/h and ℓ_2/h. The results are

$$\begin{aligned} \frac{\ell_1}{h} &= \frac{\sin(\theta_{1_{\max}} - \theta_{2_{\max}}) + \epsilon_r^{\frac{1}{2}}\sin(\theta_{2_{\max}}) - \sin(\theta_{1_{\max}})}{(\epsilon_r^{\frac{1}{2}} - 1)\sin(\theta_{1_{\max}})\sin(\theta_{2_{\max}})} \\ \frac{\ell_2}{h} &= \frac{\epsilon_r^{\frac{1}{2}}\left[\sin(\theta_{1_{\max}} - \theta_{2_{\max}}) + \sin(\theta_{2_{\max}})\right] - \sin(\theta_{1_{\max}})}{(\epsilon_r^{\frac{1}{2}} - 1)\sin(\theta_{1_{\max}})\sin(\theta_{2_{\max}})} \end{aligned} \tag{5.7}$$

Thus ℓ_1 and ℓ_2 are determined once $\theta_{1_{\max}}$, $\theta_{2_{\max}}, \epsilon_r$ and h are known. We can then use, once more, the transit time condition to obtain θ_2 as a function of θ_1, (regarding $\epsilon_r, \ell_2/\ell_1$ as known), and thereby determine the lens boundary curve, which in general is a quartic curve.

To find θ_2 as a function of θ_1 we obtain a quadratic equation in either $\cos(\theta_2)$ or $\sin(\theta_2)$ from (5.3), which we rewrite in the form

$$\begin{aligned} B\left[\sin(\theta_1)\cos(\theta_2) - \cos(\theta_1)\sin(\theta_2)\right] &= A[\sin(\theta_1) - \epsilon_r^{\frac{1}{2}}\sin(\theta_2)] \\ A = (\ell_2/\ell_1) - 1, \qquad B &= (\ell_2/\ell_1) - \epsilon_r^{\frac{1}{2}}\,. \end{aligned} \tag{5.8}$$

Algebraic manipulations then yield a quadratic in $\cos(\theta_2)$, and the quadratic formula then yields

$$\cos(\theta_2) = \frac{AB\sin^2(\theta_1) + |B\cos(\theta_1) - A\epsilon_r^{\frac{1}{2}}|\sqrt{\left[B^2 - 2AB\epsilon_r^{\frac{1}{2}}\cos(\theta_1) + A^2\epsilon_r\right] - A^2\sin^2(\theta_1)}}{B^2 - 2AB\epsilon_r^{\frac{1}{2}}\cos(\theta_1) + A^2\epsilon_r} \tag{5.9}$$

Similarly, from a quadratic in $\sin(\theta_2)$ we may obtain

$$\sin(\theta_2) = \frac{A(A\epsilon_r^{\frac{1}{2}} - B\cos(\theta_1)) + |B|\sin(\theta_1)\sqrt{\left[B^2 - 2AB\epsilon_r^{\frac{1}{2}}\cos(\theta_1) + A^2\epsilon_r\right] - A^2\sin^2(\theta_1)}}{B^2 - 2AB\epsilon_r^{\frac{1}{2}}\cos(\theta_1) + A^2\epsilon_r} \tag{5.10}$$

Finally, to obtain the lens boundary curve we need to compute the coordinates z and Ψ as a function of θ_2 (and θ_1). The geometry in Fig. 1.2 then yields the results

$$z = \frac{(\ell_2 - \ell_1)\tan(\theta_1)}{\tan(\theta_1) - \tan(\theta_2)} \tag{5.11}$$

$$\Psi = z\tan(\theta_2) = \frac{(\ell_2 - \ell_1)\tan(\theta_1)\tan(\theta_2)}{\tan(\theta_1) - \tan(\theta_2)} \tag{5.12}$$

The case $\theta_{1_{max}} = \pi/2$ leads to some simplification in the above formulas. We find, for example, that when $\theta_{1_{max}} = \pi/2$,

$$\frac{\ell_2}{\ell_1} = \frac{\epsilon_r^{\frac{1}{2}}[\cos(\theta_{2_{max}}) + \sin(\theta_{2_{max}})] - 1}{\cos(\theta_{2_{max}}) + \epsilon_r^{\frac{1}{2}}\sin(\theta_{2_{max}}) - 1} \tag{5.13}$$

$$\frac{\ell_1}{h} = \frac{\cos(\theta_{2_{max}}) + \epsilon_r^{\frac{1}{2}}\sin(\theta_{2_{max}}) - 1}{(\epsilon_r^{\frac{1}{2}} - 1)\sin(\theta_{2max})} \tag{5.14}$$

$$\frac{\ell_2}{h} = \frac{\epsilon_r^{\frac{1}{2}}[\cos(\theta_{2_{max}}) + \sin(\theta_{2max})] - 1}{(\epsilon_r^{\frac{1}{2}} - 1)\sin(\theta_{2_{max}})} \tag{5.15}$$

and the coordinates (z, Ψ) are as given in (5.11) and (5.12). When $\theta_1 \to \theta_2 \to 0$ we find

$$\begin{aligned} \frac{\sin(\theta_2)}{\sin(\theta_1)} &\to \frac{\ell_1}{\ell_2} \\ \frac{\tan(\theta_2)}{\tan(\theta_1)} &\to \frac{\ell_1}{\ell_2} \\ z &\to \ell_2 \\ \Psi &\to 0 \end{aligned} \tag{5.16}$$

as expected.

Numerical results are obtainable from the preceding analysis. In Figures 5.1 through 5.3 we show various lens boundaries corresponding to values of F/D corresponding to 0.3, 0.4, and 0.5 respectively. As expected, we obtain larger lenses for larger values of F/D. In Figure 5.2, the results obtained correspond to the choice of F/D = 0.4. For this value, $\theta_{2_{max}} = 64.01°$, and lens boundary curves are obtained for choices of $\theta_{1_{max}}$ equal to $70°, 80°, 90°$ as well as $\theta_{2_{max}}$ itself. In Tables 5.1, 5.2, and 5.3 numerical data is presented for the case $\theta_{1_{max}} = 90°$ with F/D = 0.3, 0.4, and 0.5 by allowing θ_1 and θ_2 to vary up to their maximum values and calculating the coordinates z/h and Ψ/h.

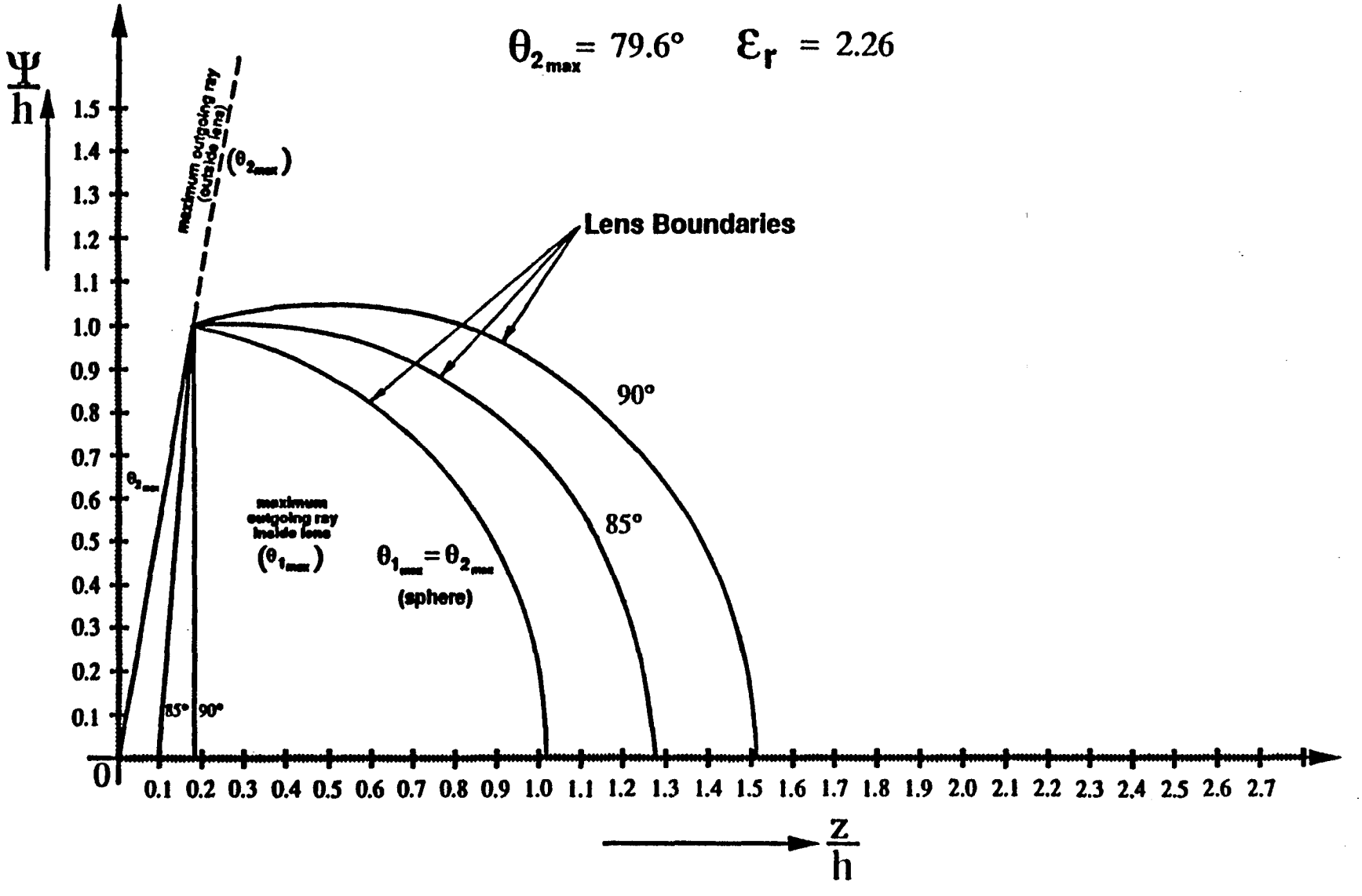

Fig. 5.1: Lens Shape for F/D = 0.3

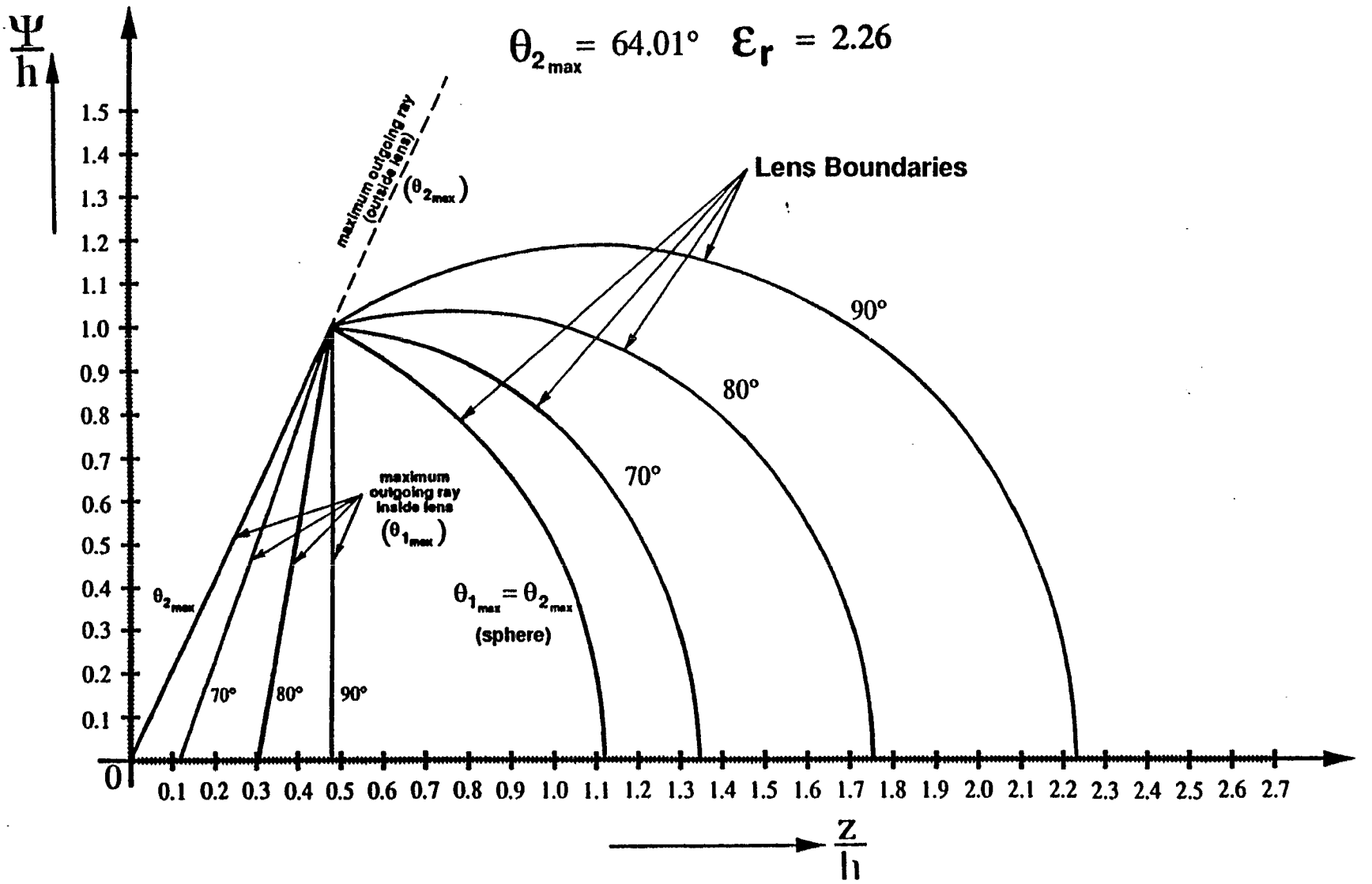

Fig. 5.2: Lens Shape for $F/D = 0.4$

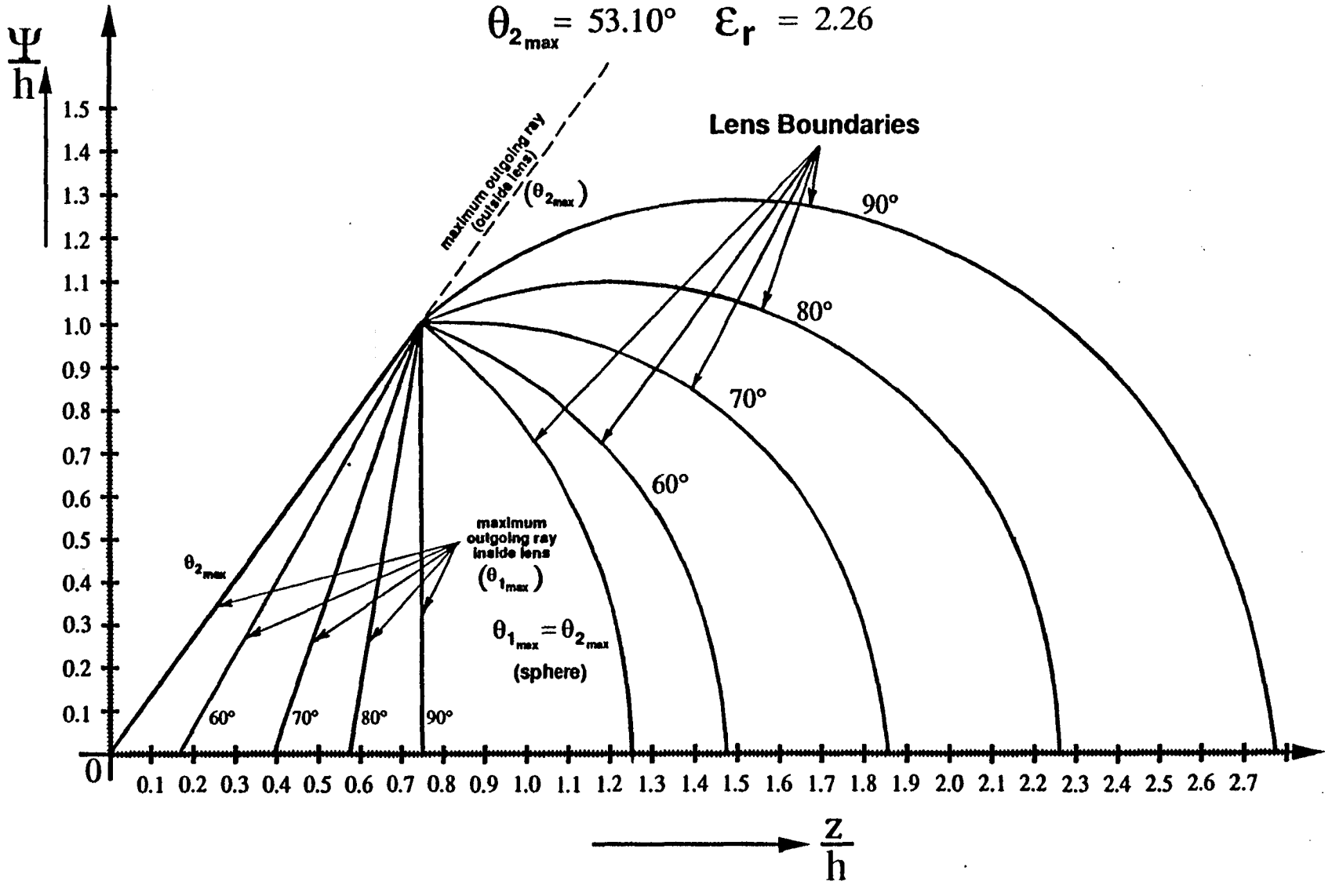

Fig. 5.3: Lens Shape for $F/D = 0.5$

θ_1	θ_2	z/h	Ψ/h
.000	.000	1.517	.000
3.000	2.636	1.514	.070
6.000	5.272	1.508	.139
9.000	7.909	1.496	.208
12.000	10.545	1.481	.276
15.000	13.182	1.461	.342
18.000	15.818	1.436	.407
21.000	18.455	1.408	.470
24.000	21.093	1.378	.531
27.000	23.730	1.340	.589
30.000	26.368	1.301	.645
33.000	29.007	1.258	.697
36.000	31.646	1.212	.747
39.000	34.286	1.164	.793
42.000	36.927	1.112	.836
45.000	39.569	1.059	.875
48.000	42.213	1.004	.911
51.000	44.858	.947	.942
54.000	47.505	.888	.970
57.000	50.154	.829	.993
60.000	52.805	.769	1.013
63.000	55.460	.708	1.029
66.000	58.118	.647	1.040
69.000	60.780	.586	1.048
72.000	63.446	.526	1.052
75.000	66.118	.466	1.052
78.000	68.795	.407	1.048
81.000	71.479	.349	1.041
84.000	74.171	.292	1.031
87.000	76.872	.237	1.017
90.000	79.583	.184	1.000

Table 5.1: Lens Shape Data for $F/D = 0.3$, with $0 \leq \theta_1 \leq \theta_{1max}$ and $0 \leq \theta_2 \leq \theta_{2max}$ and $\theta_{1max} = 90°$, $\theta_{2max} = 79.6°$, $\varepsilon_r = 2.26$

θ_1	θ_2	z/h	Ψ/h
.000	.000	2.236	.000
3.000	2.345	2.232	.091
6.000	4.690	2.222	.182
9.000	7.032	2.205	.272
12.000	9.371	2.181	.360
15.000	11.706	2.151	.446
18.000	14.036	2.115	.529
21.000	16.359	2.073	.608
24.000	18.675	2.025	.684
27.000	20.981	1.972	.756
30.000	23.278	1.914	.823
33.000	25.563	1.851	.886
36.000	27.836	1.785	.943
39.000	30.093	1.715	.994
42.000	32.335	1.642	1.040
45.000	34.560	1.567	1.080
48.000	36.764	1.490	1.113
51.000	38.947	1.412	1.141
54.000	41.107	1.332	1.163
57.000	43.240	1.253	1.178
60.000	45.345	1.173	1.188
63.000	47.418	1.095	1.191
66.000	49.457	1.017	1.189
69.000	51.458	.941	1.182
72.000	53.417	.867	1.169
75.000	55.331	.796	1.151
78.000	57.196	.728	1.129
81.000	59.005	.662	1.102
84.000	60.753	.600	1.072
87.000	62.435	.542	1.039
90.000	64.044	.488	1.002

Table 5.2: Lens Shape Data for F/D = 0.4, with $0 \leq \theta_1 \leq \theta_{1max}$ and $0 \leq \theta_2 \leq \theta_{2max}$ and $\theta_{1max} = 90°$, $\theta_{2max} = 64.0°$, $\varepsilon_r = 2.26$

θ_1	θ_2	z/h	Ψ/h
.000	.000	2.748	.000
3.000	2.180	2.743	.104
6.000	4.358	2.731	.208
9.000	6.532	2.710	.310
12.000	8.700	2.681	.410
15.000	10.861	2.644	.507
18.000	13.011	2.600	.601
21.000	15.150	2.548	.690
24.000	17.274	2.490	.774
27.000	19.381	2.425	.853
30.000	21.469	2.355	.926
33.000	23.536	2.280	.993
36.000	25.577	2.200	1.053
39.000	27.591	2.117	1.106
42.000	29.574	2.031	1.152
45.000	31.523	1.942	1.191
48.000	33.433	1.851	1.222
51.000	35.301	1.760	1.246
54.000	37.122	1.668	1.263
57.000	38.891	1.577	1.272
60.000	40.604	1.486	1.274
63.000	42.254	1.398	1.270
66.000	43.836	1.311	1.259
69.000	45.342	1.228	1.243
72.000	46.767	1.147	1.220
75.000	48.102	1.071	1.193
78.000	49.339	.998	1.162
81.000	50.471	.929	1.126
84.000	51.488	.865	1.087
87.000	52.382	.806	1.045
90.000	53.143	.751	1.002

Table 5.3: Lens Shape Data for F/D = 0.5, with $0 \leq \theta_1 \leq \theta_{1max}$ and $0 \leq \theta_2 \leq \theta_{2max}$ and $\theta_{1max} = 90°$, $\theta_{2max} = 53.1°$, $\varepsilon_r = 2.26$

6 Concluding Remarks

It has been noted that one significant application of the type of dielectric lens discussed here is its possible use for launching an approximation to a spherical TEM wave onto an IRA. As one goes to higher and higher voltage pulses launched onto the TEM feed, the possibility of electrical breakdown is a consideration. The desire for faster and faster pulse rise times means that one needs to establish the TEM-mode field distribution over the cross section of the feed. In this case one would require that such pulses be treated as waves, and one in general wants to match these waves from one region to another with a minimum of distortion and reflection.

The lenses considered here have been treated from an "equal-time" point of view. Thus some reflections are introduced at boundaries. However, these reflections can be small in certain cases, and the wave passing into the second medium can approximate a dispersionless TEM wave. Future investigations will take up the issue of impedance matching.

References

[1] C. E. Baum, Radiation of Impulse-Like Transient Fields, Sensor and Simulation Note 321, November 1989.

[2] C. E. Baum, Configurations of TEM Feed for an IRA, Sensor and Simulation Note 327, April 1991.

[3] C. E. Baum, Wedge Dielectric Lenses for TEM Waves Between Parallel Plates, Sensor and Simulation Note 332, September 1991.

[4] C. E. Baum, J. J. Sadler, and A. P. Stone, A Prolate Spheroidal Uniform Isotropic Dielectric Lens Feeding a Circular Coax, Sensor and Simulation Note 335, December 1991.

[5] C. E. Baum, J. J. Sadler and A. P. Stone, Uniform Isotropic Dielectric Equal-Time Lenses for Matching Combinations of Plane and Spherical Waves, Sensor and Simulations Note 352, December 1992.

[6] C. E. Baum, J. J. Sadler, and A. P. Stone, Uniform Wedge Dielectric Lenses for Bends in Circular Coaxial Transmission Lines, Sensor and Simulations Note 356, December 1992.

[7] C. E. Baum and A. P. Stone, *Transient Lens Synthesis: Differential Geometry in Electromagnetic Theory,* Hemisphere Publishing Corp., 1991.